Nuclear polarization in muonic ^{90}Zr

T. Q. Phan, P. Bergem, A. Rüetschi,* L. A. Schaller, and L. Schellenberg
Institut de Physique, Université de Fribourg, CH-1700 Fribourg, Switzerland
(Received 8 April 1985)

The energies of muonic x-ray transitions sensitive to the nuclear charge parameters have been measured with a precision up to 9 ppm in muonic ^{90}Zr. Combining our muonic-atom results for the equivalent nuclear charge radii $R_{k,\alpha}$ with recent elastic electron scattering data, the rms radius of ^{90}Zr could be determined as $\langle r^2\rangle^{1/2}=4.2726(9)$ fm. In addition to the nuclear monopole charge distribution, nuclear polarization correlations between the muonic $1s$ and $2s$ and the $1s$ and the two $2p$ states could be determined. With additional constraints from elastic electron scattering and theory, the nuclear polarization corrections of the four lowest-lying states could be evaluated with precisions of the order of 15%. Of particular significance is the result for the two $2p$ states, because the experimentally determined $2p_{1/2}$ correction is smaller than the nuclear polarization correction in the $2p_{3/2}$ state, in contrast to current theoretical models.

I. INTRODUCTION

The calculations of the nuclear polarization corrections in muonic atoms are known to be difficult.[1] The lack of knowledge of the complete spectrum of nuclear excited states, both discrete and continuous ones, demands the use of specific nuclear models and leads to different results depending on the approximations used. Typical quoted uncertainties range from 10 to 50%. These uncertainties in the nuclear polarization calculations limit at present the accuracy with which absolute nuclear charge moments can be deduced from muonic-atom transition energies. Most calculations so far have been performed for the heavy, doubly-magic nucleus ^{208}Pb,[2–5] but experimental confirmations are largely missing. A recent study of muonic ^{208}Pb (Ref. 6) employing the data of Kessler *et al.*[7] revealed a discrepancy between theory and experiment. In particular, several experimental correlations between the nuclear polarization corrections in the low-lying muonic states of ^{208}Pb are in disagreement with theory, suggesting a fundamental problem in present theoretical approaches to the nuclear polarization effect.

In order to study this problem further, and specifically, in order to find out whether such an effect is systematic, it is important to extend the measurements to lighter muonic atoms. Former muonic-atom measurements on the nuclei ^{208,206}Pb, ^{142,140}Ce, ^{138}Ba, and ^{120}Sn (Refs. 8–10) did not arrive at definitive conclusions, due to lack of precision. The present work deals for the first time with a medium-A nucleus, the semimagic nucleus ^{90}Zr. In order to obtain a sufficient number of nuclear parameters, all transitions sensitive to the finite nuclear charge extension have to be measured. In particular, muonic transitions to and from the weakly populated $2s$ state must be included. This state has, next to the $1s$ state, the largest overlap with the nucleus. In addition, the muonic $2s$ wave function happens to be zero at the edge of the nuclear surface of ^{90}Zr. Hence, it is sensitive to the interior of that charge distribution. However, due to the low population of the $2s$ state, transitions to and from this state are difficult to be precisely determined. In particular, there is a large Compton background from more energetic and strongly populated circular transitions. In order to suppress this background, we have employed an anti-Compton spectrometer.

From the present measurements, correlations between the nuclear polarization corrections of different muonic states will be deduced. Using a nuclear model, constraints from the analysis of recent elastic electron scattering data[11] and theoretical nuclear polarization corrections for the $n=3$ (and higher) muonic states,[12,13] it will be shown that the nuclear polarization corrections of the $1s$, $2s$, $2p_{1/2}$, and $2p_{3/2}$ levels can be determined with precisions of the order of 15%. A comparison of the present results with theoretical calculations exhibits the same kind of discrepancy as does the muonic ^{208}Pb experiment.[6] Preliminary data regarding the present ^{90}Zr as well as a new ^{208}Pb experiment have been communicated at conferences.[14,15]

Section II summarizes the theoretical background concerning the interpretation of muonic transition energies and emphasizes specifically the role of nuclear polarization corrections. Section III describes the experimental setup at the superconducting muon channel of SIN and the performance of our anti-Compton spectrometer. Also included in this section is the calibration method used to determine precise muonic transition energies. The analysis with regard to the nuclear charge parameters is treated in Sec. IV. Results in terms of nuclear polarization correlations, nuclear polarization corrections, and the nuclear rms radius of ^{90}Zr are presented. Finally, Sec. V compares the experimental results with theory and stresses in particular the discrepancy found for the sign of the nuclear polarization correction to the $2p$ splitting.

II. THEORY

In order to determine the nuclear charge parameters, the measured muonic transition energies have to be compared with calculations starting with the Dirac equation

for a static nucleus. In addition to the electromagnetic level shifts produced by the static, finite nuclear charge distribution, there are additional shifts associated with dynamical excitations of the nucleus. They are known as nuclear polarization corrections. Due to the spin zero of the ^{90}Zr ground state, the dynamic hyperfine structure effects are negligible. Because of the well-known difficulties associated with the solution of the relativistic bound state problem, one depends in a practical way upon a Hamiltonian formalism in which each physically important effect is represented by an effective, separable potential. These effective potentials are generally added to the Dirac equation in a perturbative way. Hence, we write the total Hamiltonian of the muon-nucleus system as

$$\mathcal{H}=H_\mu+H_N+V_0+(V-V_0)=H_0+V_R \ ,$$

where H_0 is the zero-order Hamiltonian, the sum of a relativistic muon Hamiltonian H_μ and a nuclear Hamiltonian H_N. The eigenfunctions of H_0 are products of muonic and nuclear wave functions. Included in H_0 is a static central potential V_0 as seen by the muon. It represents the average electrostatic potential generated by the extended nucleus,

$$V_0(\mathbf{r}_\mu)=\langle 0||-Z\alpha\int\frac{\rho(\mathbf{r}_N)}{|\mathbf{r}_\mu-\mathbf{r}_N|}d^3r_N||0\rangle \ .$$

Furthermore, the muonic part of H_0, H_μ, is assumed to include all corrections not involving nuclear excitations and static nuclear moments. These corrections are the different orders of the electron-positron vacuum polarization, the $\mu^-\mu^+$ and the hadronic vacuum polarizations, the anomalous magnetic moment, the Lamb shift, i.e., first- and second-order vertex corrections, the relativistic recoil, and the electron screening.[1] For muonic ^{90}Zr, these different corrections are listed in Table I together with the finite size binding energies. The latter were evaluated using for $V_0(\mathbf{r}_\mu)$ a spherically symmetric Fermi-type charge distribution, with the half-density radius c and the diffuseness parameter a obtained from a least-squares fitting procedure (see Sec. IV).

The residual muon-nuclear interaction $V_R=V-V_0$ will change the unperturbed wave functions of the muon and the nucleus by admixing or virtually exciting other states. This normally results in an increase of the binding energy of the total system. The nucleus therefore does not simply act as a rigid charge distribution, but responds dynamically to the electromagnetic muon probe. Such polarization effects may be described as virtual excitations of nuclear states by the muon. The deexcitation of these states to the ground state transfers energy back to the probe. The muonic cascade does not result in real final state excitations of the nucleus, but proceeds between the different muonic atom levels which are displaced by the virtual excitations from the positions they would have occupied for a rigid nucleus.

The nuclear polarization energy shift (NP) is calculated in second order as

$$\Delta E^i_{\rm NP}=\sum_{j\neq i}\frac{|\langle j|V_R|i\rangle|^2}{E_i-E_j} \ ,$$

where $|i\rangle$ is a particular muon state coupled to the nuclear ground state, and the states $|j\rangle$ represent the entire spectrum of all other muonic and excited nuclear states. The different muon states are treated by a reference spectrum method,[3] the high-lying nuclear states by energy-weighted sum rules.[13] The energy shifts $\Delta E^i_{\rm NP}$ for the low-lying muonic levels ($i\leq 3$) are calculated using the computer codes RURP (Ref. 16) and MUON (Ref. 17). Table II shows detailed results of such theoretical nuclear polarization calculations for the muonic $1s$, $2s$, $2p_{1/2}$, $2p_{3/2}$, $3p_{1/2}$, and $3p_{3/2}$ states in ^{90}Zr. Regarding the continuous, high-lying nuclear spectrum, the isoscalar and/or isovector contributions for multipoles of order $0\leq\lambda\leq 4$ are listed. For each multipole, the strength is concentrated in a single resonant state whose energy is reproduced by an empirical expression and whose strength is given by energy-weighted sum rules. Also included in Table II are electric monopole, quadrupole, and octupole contributions of the low-lying nuclear states using the known excitation

TABLE I. Corrections to muon binding energies for ^{90}Zr (in keV).

State	Finite size binding energy (a)	Vacuum polarization (b)	(c)	Lamb shift (d)	Other corrections (e)
$1s_{1/2}$	3642.965	25.750	0.137	−1.231	0.151
$2s_{1/2}$	1021.254	4.989	0.020	−0.209	0.023
$2p_{1/2}$	1147.770	5.939	0.003	−0.001	0.012
$2p_{3/2}$	1126.996	5.621	0.002	−0.040	0.012
$3p_{1/2}$	507.998	1.818	0.001	−0.003	0.011
$3p_{3/2}$	502.049	1.735	0.000	−0.014	0.010
$3d_{3/2}$	503.086	1.438	0.000	−0.003	0.008
$3d_{5/2}$	500.690	1.411	0.000	−0.002	0.008

[a]The parameters c and a of the first column of Table VII were used in these calculations, together with the theoretical nuclear polarization corrections of Table II.
[b]All orders.
[c]$\mu^+\mu^-$ vacuum polarization and hadronic vacuum polarization.
[d]First- and second-order vertex corrections, including anomalous magnetic moment.
[e]Relativistic recoil and electron screening corrections.

TABLE II. Nuclear polarization (NP) corrections (in eV). Upper half: The states I_S^P, I_V^P are isoscalar (S) and isovector (V) giant resonance states. Their respective excitation energies are estimated using an empirical formula. The strength of each electric multipole is determined by sum rules (Ref. 13). Lower half: Low-lying excited states whose reduced transition probabilities are precisely known (Refs. 18 and 19).

			$1s_{1/2}$		$2s_{1/2}$		$2p_{1/2}$		$2p_{3/2}$		$3p_{1/2}$		$3p_{3/2}$	
λ	E_{exc} (MeV)	$B(E\lambda)$ (e^2b^λ)	S	V	S	V	S	V	S	V	S	V	S	V
0^+			147	81	25	13	1	1	1	0	0	0	0	0
1^-				395		49		34		30		10		9
2^+			178	72	22	9	12	4	11	4	4	0	4	0
3^-			16	13	2	2	1	1	1	1	1	0	1	0
4^+			8	5	1	0	0	0	0	0	0	0	0	0
0^+	1.76	0.000 07	4		0		0		0		0		0	
2^+	2.18	0.065 30	73		9		9		9		3		3	
2^+	3.31	0.007 84	8		1		1		1		0		0	
2^+	3.84	0.022 40	23		3		2		2		2		2	
3^-	2.75	0.084 21	40		5		3		2		1		1	
3^-	5.65	0.006 74	3		0		0		0		0		0	
3^-	5.78	0.001 41	1		0		0		0		0		0	
NP (total)			1067		141		69		62		21		20	

energies E_{exc} and transition strengths $B(E\lambda)$ of these states.[18,19]

III. EXPERIMENT

A. Experimental setup and spectra

The experiment has been performed at the superconducting $\mu E1$ channel of the SIN ring accelerator at Villigen, Switzerland. The primary proton beam had an intensity of 120 μA, the selected pion momentum was 150 MeV/c, and the momentum of the backward decaying muons 85 MeV/c. Typical stopped muon rates in a target of effective thickness 0.49 g/cm^2 were 600 000/s as measured by a $123\bar{4}$ coincidence in the telescope counters. The target consisted of 11g $^{90}ZrO_2$ powder enriched to 99.36% (see Table III). The muonic x-ray radiation and the delayed nuclear γ rays were detected by a total of three semiconductor counters, namely a 2 cm^3 planar Ge(Li) diode with a resolution of 700 eV (FWHM) at 122 keV, an intrinsic Ge detector of size 65 cm^3 and of resolution 1.75 keV at 1332 keV, and a 90 cm^3 coaxial Ge(Li) detector with a resolution of 2.0 keV at 1332 keV. In general, setup and electronics were similar to former runs.[20,21] Special shielding, however, was required for the Compton suppression spectrometer. This spectrometer consists of the 65 cm^3 intrinsic Ge detector, an inversely drifted, n-type coaxial detector, surrounded in an asymmetrical way by a NaI(Tl) annulus of diameter 22 cm and length 29 cm.[15,22] Under beam conditions and in the energy range of interest (50—700 keV), an average Compton reduction factor of 3—4 has been obtained. Figures 1(b)—(d) show the circular $3d$-$2p$ as well as the weakly populated $3p$-$2s$ and $2s$-$2p$ transitions taken with our anti-Compton spectrometer. The peak-to-background ratios of the latter two transitions are of the order of 1:1 or better. Without Compton suppression, there would be a large background from transitions between strongly populated circular orbits with higher energies ($2p$-$1s$, $3d$-$2p$, and $4f$-$3d$). Hence, it would not have been possible to obtain the required precision in energy. Also shown in Fig. 1 [Fig. 1(a)] are the two high-energetic $2p$-$1s$ transitions in muonic ^{90}Zr taken with the 65 cm^3 detector without anti-Compton suppression. All spectra in Fig. 1 are parts of so-called "prompt" spectra, i.e., spectra taken in prompt coincidence with a stopped muon. Calibration spectra were recorded for a time period of 200 ns, but only if an arriving muon was not stopped in the target ($12\Lambda123\bar{4}$ coincidence). In this way, the beam loading could be closely reproduced. The different calibration sources together with their respective transition energies and uncertainties are listed in Table IV.[21,23–25] The sources were located in such a way as to ensure an irradiation of the Ge detectors similar to that from the enriched ^{90}Zr target. Finally, spectra were recorded within 20—120 ns after a stopped muon. These spectra contain preferentially delayed nuclear γ rays, i.e., γ rays originating after weak nuclear muon capture in ^{90}Zr. They also show calibration peaks feeding through by accidental coincidences. The strongest calibration lines appear in addition in the prompt spectra which had a time window of 20 ns width. Inelastic neutron scattering could induce further prompt peaks. However, the chances of accidental degeneracy of muonic transitions with prompt nuclear deexcitation γ lines are negligible, since the first excited state of the semimagic ^{90}Zr nucleus lies 1.76 MeV above its ground state, and the level density of ^{90}Zr below a few MeV is low.

TABLE III. Target mass and isotopic composition.

Material	Amount (g)	Isotopic abundance (%) ^{90}Zr	^{91}Zr	^{92}Zr	^{94}Zr	^{96}Zr
^{90}Zr	11	99.36	0.30	0.17	0.12	0.04

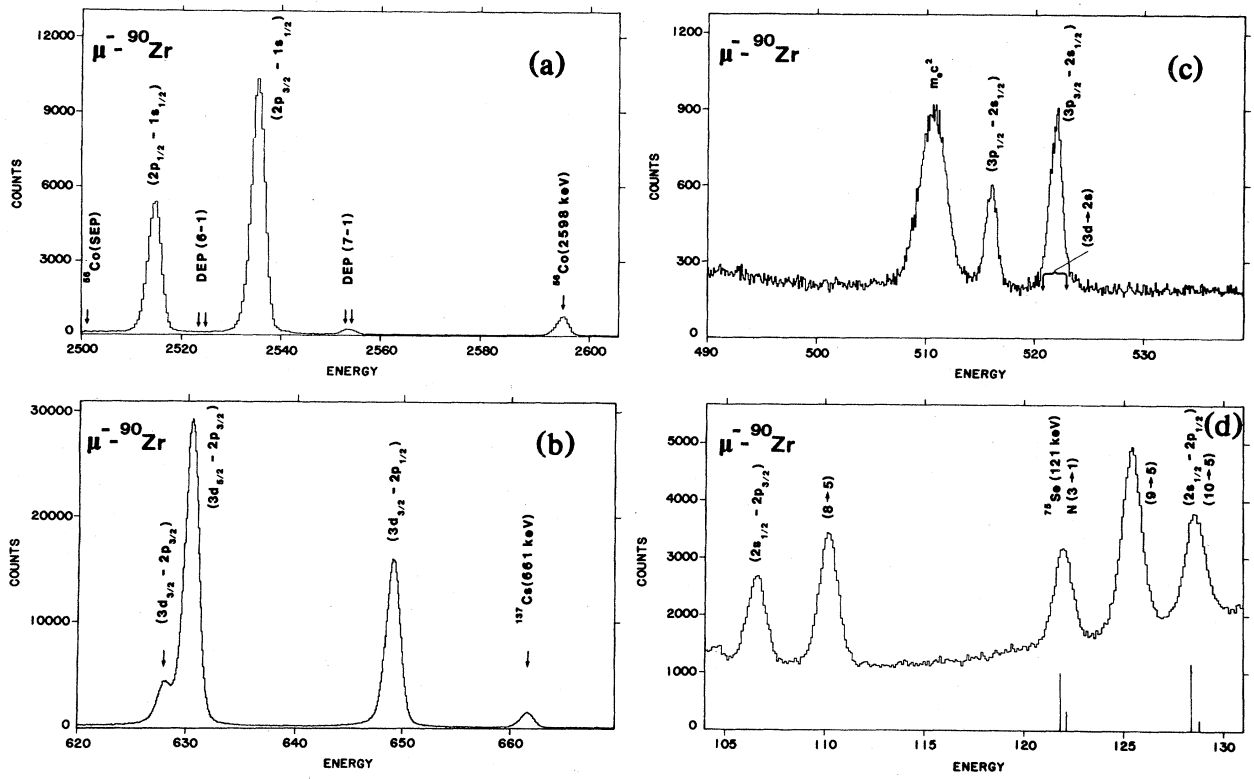

FIG. 1. Muonic x-ray spectra of ^{90}Zr showing regions of the $2p$-$1s$ [(a), upper left], $3d$-$2p$ [(b), lower left], $3p$-$2s$ [(c), upper right], and $2s$-$2p$ [(d), lower right] transitions. The spectra of (b)—(d) were taken with the anti-Compton spectrometer. The energies are given in keV.

TABLE IV. Sources with their principal lines used for energy calibration.

Source	Ref.	Energies (keV)
^{12}C(μ^- x rays)	21	75.263(5), 89.217(6)
^{16}O(μ^- x rays)	23	133.528(15), 158.412(15)
^{75}Se	25	66.060(7), 96.734(2), 121.119 (3), 136.002(3), 198.596(6), 264.656(4), 279.538(3), 303.924(3), 400.657(2)
^{192}Ir	25	136.343(1), 205.796(1), 295.958(1), 308.457(1), 316.508(1), 416.472(1), 468.072(1), 484.578(1), 588.585(2), 604.415(2), 612.466(2)
^{228}Th	25	2614.533(13)
^{144}Ce	25	2185.662(7)
^{56}Co	25	2015.179(11), 2034.759(11), 2113.107(12), 2212.921(10), 2598.460(10), 3009.596(17), 3201.954(14), 3253.417(14)
^{137}Cs	25	661.660(3)
^{152}Eu	25	244.699(1), 344.281(2)
^{195}Au	24	98.857(10), 129.735(10)

B. Transition energies

For a successful determination of both the nuclear charge parameters and the nuclear polarization corrections of the low-lying muonic levels in ^{90}Zr, the highest attainable precision in the respective transition energies is mandatory. The procedure employed in order to obtain this aim was the following.

First, we selected isolated calibration and muonic x-ray photopeaks in the three differently time-gated spectra and applied the computer code LINFIT (Ref. 20) in order to determine the respective center-of-gravity positions. The so obtained asymmetry parameters were plotted as a smooth function of energy and the peaks were then again fitted using such average parameters. The same method was applied to the line widths (FWHM) which increase essentially with the square root of the energy. The mean parameters were then employed for the fits of all calibration and muonic x-ray peaks. In order to convert the peak positions to energies, a linear relationship between positions and energies was assumed. The remaining nonlinearity of our measuring system was determined from the well-spaced calibration line positions in the calibration spectra. Since the nonlinearity behavior is the same in the different on-line spectra,[26] it can also be used for the prompt spectra. Furthermore, we have found no shifts between the prompt and the calibration spectra within the limits of the statistical errors. The experimental muonic x-ray energies obtained by such a calibration procedure had to be corrected for the known isotopic abundances of the other stable Zr isotopes, i.e., ^{91,92,94,96}Zr (see Table III) using the isotope shifts measured by Emrich *et al.*[27] Finally, the energies of the emitted muonic x rays were transformed into transition energies by adding the recoil energy of the atom. Table V shows the obtained transition energies involving the $1s$, $2s$, $2p$, $3p$, and $3d$ states in muonic ^{90}Zr. In the energy range below 1 MeV, the data were taken with the anti-Compton spectrometer. In addition, the $2s$-$2p_{1/2}$ and $2s$-$2p_{3/2}$ transitions were also obtained with the small 2 cm^3 detector. The high energy data were taken with the 65 cm^3 detector alone, since the anti-Compton efficiency becomes lower with increasing energy. The spectra obtained with the 90 cm^3 detector served for consistency purposes. The quoted errors of Table V take the nonlinearity errors as well as the absolute uncertainties of the calibration lines into account. The next table, Table VI, shows the very good internal consistency obtained in the splittings of the $2p$ ($\Delta 2p$) and $3p$ ($\Delta 3p$) levels. The small error in the $2p$ splitting is especially important when discussing our results in terms of the nuclear polarization shifts (see the following sections).

TABLE V. Experimental energies (keV) and errors (eV) of muonic transitions involving the $1s$, $2s$, $3p$, and $3d$ levels in ^{90}Zr. [The uncertainty in the correction for nonlinearity and the absolute error of the calibration energies (see Table IV) have been included in the quoted errors of the muonic transition energies.]

Transition	Experimental energy
$2s_{1/2}\rightarrow 2p_{3/2}$	106.404(9)[a]
$2s_{1/2}\rightarrow 2p_{1/2}$	127.525(12)[a]
$3p_{1/2}\rightarrow 2s_{1/2}$	516.419(17)
$3p_{3/2}\rightarrow 2s_{1/2}$	522.470(24)
$3d_{3/2}\rightarrow 2p_{3/2}$	628.112(12)
$3d_{5/2}\rightarrow 2p_{3/2}$	630.533(9)
$3d_{3/2}\rightarrow 2p_{1/2}$	649.229(10)
$2p_{1/2}\rightarrow 1s_{1/2}$	2515.122(23)
$2p_{3/2}\rightarrow 1s_{1/2}$	2536.237(22)
$3p_{1/2}\rightarrow 1s_{1/2}$	3158.998(70)
$3p_{3/2}\rightarrow 1s_{1/2}$	3165.100(70)

[a]Average values obtained from measurements with the 2 cm^3 and the 65 cm^3 detectors.

IV. RESULTS

The present section utilizes the muonic-atom transition energies listed in Table V in order to deduce the nuclear charge parameters including the nuclear polarization and the nuclear rms radius.

A. Nuclear polarization and charge parameters

Both charge parameters and nuclear polarization corrections have to be determined simultaneously from the data. Hence, correlations between the different parameters have to be carefully studied. Nevertheless, important general conclusions regarding the relative sizes of the NP corrections in several low-lying muonic states can be obtained, as has been shown by Yamazaki *et al.*[6] in the case of lead.

TABLE VI. Internal consistency checks of experimental muonic transition energies.

Level difference	Transitions	Energy (keV)	Adopted value (keV)
$\Delta(2p)$	$(2p_{3/2}\text{-}1s_{1/2})-(2p_{1/2}\text{-}1s_{1/2})$	21.115(18)	
	$(2s_{1/2}\text{-}2p_{1/2})-(2s_{1/2}\text{-}2p_{3/2})$	21.121(11)	
	$(3d_{3/2}\text{-}2p_{1/2})-(3d_{3/2}\text{-}2p_{3/2})$	21.117(12)	21.118(8)
$\Delta(3p)$	$(3p_{3/2}\text{-}2s_{1/2})-(3p_{1/2}\text{-}2s_{1/2})$	6.051(29)	
	$(3p_{3/2}\text{-}1s_{1/2})-(3p_{1/2}\text{-}1s_{1/2})$	6.102(95)	6.052(28)
$3p_{3/2}\text{-}1s$	$(3p_{3/2}\text{-}2s_{1/2})+(2s_{1/2}\text{-}2p_{3/2})+(2p_{3/2}\text{-}1s_{1/2})$	3165.111(34)	
	$(3p_{3/2}\text{-}1s_{1/2})$	3165.100(70)	

The specific choice of the nuclear charge distribution is not the determining factor in the analysis of the data, since the muonic transition energies are sensitive to certain nuclear charge moments only, as will be discussed in Sec. IV B. The nucleus ^{90}Zr studied in the present work is a semimagic nucleus with ground state spin zero. Hence, a spherical, two-parameter Fermi distribution with half-density radius c and diffuseness parameter a has been inserted into the potential of the Dirac equation. The program MUON2, in combination with the computer code XRAY2,[17] has been employed in order to compare the experimental with the theoretical transition energies.

In particular, we have determined the experimental correlations between the nuclear polarization corrections for the $1s$ and $2s$ states and for the $1s$ state and the $2p$ fine structure splitting. The experimentally allowed values of the NP corrections for the $1s$ and $2s$ states were obtained by varying the quantities c, a, and NP$2s$ for different NP$1s$ values. The NP$2s$ corrections corresponding to each χ^2 minimum for a given NP$1s$ value were then plotted as a function of NP$1s$. The result is shown in Fig. 2(a). Similarly, Fig. 2(b) shows the dependence of the difference

$$\mathrm{NP}(\Delta 2p)=\mathrm{NP}2p_{1/2}-\mathrm{NP}2p_{3/2}$$

from the NP$1s$ value. Here, we have varied the quantities c, a, NP$2p_{1/2}$, and NP$2p_{3/2}$, and the plotted difference NP$(\Delta 2p)$ corresponds again to each χ^2 minimum at a given NP$1s$ value. The shaded areas in both graphs correspond to uncertainties of ± 22 and ± 3 eV, respectively. These errors have been deduced from all minimizations performed, including also other combinations of fixed and variable parameters, as will be discussed below. The results of the theoretical calculations of Rinker and Speth[13] are given as discrete points in Fig. 2. Since the nonrelativistic calculations of Chen[3] and of Skardhamar[4] are not meaningful for the $2p$ splitting, they are not included in Fig. 2.

Figure 2(a) shows essentially a one-to-one relationship between the $1s$ and the $2s$ nuclear polarizations. Such a constant ratio is predicted by theory, due to the predominance of the giant monopole resonance in spherically symmetric states with angular momentum zero.[1,13] The theoretical calculations of Rinker and Speth are consistent with the experimental results of the two s states, but not with the results between the s states and the two $2p$ states. Specifically, agreement with the theoretical value

$$\mathrm{NP}2p_{1/2}-\mathrm{NP}2p_{3/2}=+7 \text{ eV}$$

(see Table II) can only be obtained, if the nuclear polarization correction of the $1s$ state becomes larger than 3 keV. Extrapolating to the case of muonic lead, the corresponding theoretical NP correction for the $1s$ state would then amount to more than 15 keV. Such a large value seems highly unlikely, considering the theoretical values and their estimated errors as discussed in Ref. 5.

Our analysis stresses the importance to include the $2p$ levels when determining nuclear polarization corrections. Due to the precision of the present data, specifically with regard to the $2p$ fine structure splitting (see Table VI), a determination of the NP$1s$ and NP$2s$ corrections together with the two parameters c and a of the chosen Fermi-type charge distribution, using all transitions of Table V, leads to a poor fit of these experimental data and to an overestimation of the NP$1s$ and the NP$2s$ corrections, if the NP$2p$ values are taken from theory. Table VII shows that the χ^2 value considerably improves if the NP$2p$ values are fitted as free parameters. The importance of the $2p$ levels with regard to the nuclear polarization is also seen, if we

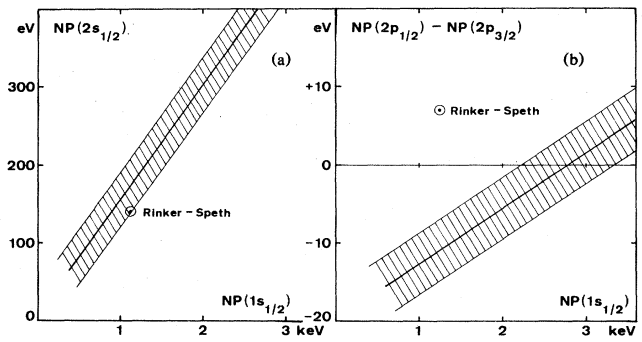

FIG. 2. Nuclear polarization correlations between the $1s$ and $2s$ states [(a), left] and between the $1s$ and the $2p$ states [(b), right] in muonic ^{90}Zr. The shaded areas correspond to estimated errors (see the text). The theoretical predictions are from Ref. 13.

TABLE VII. Nuclear parameters determined from fits to muonic transitions involving the $1s$, $2s$, $2p$, $3p$, and $3d$ levels in ^{90}Zr. This table also includes the rms radii (in fm), the theoretical and experimental $2p$ splittings (in eV), and the χ^2 values per degree of freedom. The nuclear polarization corrections are expressed in eV, the nuclear extensions in fm. Column (I) employs theoretical nuclear polarization corrections. Column (II) fits, in addition to the half-density radius c, the nuclear polarization corrections of the $1s$, $2s$, $2p_{1/2}$, and $2p_{3/2}$ states. The diffuseness parameter a is taken from elastic electron scattering data (Refs. 11 and 28). The errors of NP$2p$ are relative errors, as explained in the text. The uncertainties of NP$1s$ and NP$2s$ have been derived by quadratic addition of the statistical fit errors, the relative NP$2p$ errors, and a 50% error in NP$3p$.

Nuclear parameter	(I)	(II)
c	4.8791(8)	4.9011(2)
a	0.5367(4)	0.5272
NP$1s$	1067	1138(155)
NP$2s$	141	175(22)
NP$2p_{1/2}$	69	55(3)
NP$2p_{3/2}$	62	66(3)
NP$3p_{1/2}$	21	21
NP$3p_{3/2}$	20	20
NP$3d$	0	0
rms radius	4.2736(40)	4.2724(9)
$\Delta(2p)$cal.	21 138	21 121
$\Delta(2p)$exp.	21 118(8)	21 118(8)
χ^2	4.0	0.76

treat their dependence from the finite nuclear size and the nuclear polarization separately. Table VIII shows that the kth moments and correspondingly the equivalent radii $R_{k,\alpha}$, which will be discussed in Sec. IV B, are practically the same for the two $2p$ states. Hence, the $2p$ fine structure transitions yield the same monopole information about the nuclear charge distribution. However, this is not true for the nuclear polarization shifts. Matrix elements involving the muonic $1s$, $2s$, $2p_{1/2}$, and $2p_{3/2}$ wave functions obey quite different angular momentum selection rules, and the nucleus responds differently to deformation forces induced by different multipole excitations. Therefore, each of the muon states polarizes the nucleus in its own, unique manner, and the $2p$ splitting is not strongly correlated with the $1s$ (or $2s$) state with regard to the nuclear polarization.

The nuclear polarization correlations discussed above point to a serious problem between theory and experiment in the NP($\Delta 2p$) splitting. It is thus tempting to extend the older line of analysis[8,10] in order to deduce values for the nuclear polarization corrections of the individual levels, in particular of the lowest-lying $1s$, $2s$, $2p_{1/2}$, and $2p_{3/2}$ levels. Since the nuclear form factor and the absolute nuclear polarization corrections cannot be determined independently from the muonic-atom data alone, we need additional constraints on the free parameters. Such constraints could be obtained by combining the results of recent elastic electron scattering data on ^{90}Zr by Rothhaas[11] with our muonic-atom experiment.

The elastic electron scattering data of Rothhaas provide a nuclear charge distribution of the Fourier-Bessel form

$$\rho(r)=\begin{cases}\sum_{\nu=1}^{15} a_\nu j_0(q_\nu r) & \text{for } r\le R\\ 0 & \text{for } r>R\end{cases}.$$

In the framework of the plane-wave Born approximation, the parameters a_ν are related to the cutoff radius $R=10$ fm at momentum transfers $q_\nu=\pi\nu/R$. Knowing the coefficients a_ν from a fit to the (e,e) cross sections, the muonic binding and transition energies can be evaluated from the above charge distribution. Taking all corrections beyond finite nuclear size excepting the nuclear polarization into account, the difference in calculated and experimental binding energies can be interpreted as an experimentally determined nuclear polarization correction. The success of such a procedure depends on the smallness of the errors in both elastic electron scattering and muonic-atom data. Regarding the (e,e) measurements, no absolute normalization errors had to be included.[28] Specifically, we have calculated the equivalent radii $R_{k,\alpha}$ and their errors $\delta R_{k,\alpha}$ which correspond to the muonic $2p_{3/2}$-$1s$ and $2s$-$2p_{3/2}$ transitions, using the coefficients a_ν and their uncertainties δa_ν. The nuclear polarization correction of the $2p_{3/2}$ state was fixed at its theoretical value. The errors $\delta R_{k,\alpha}$ were transformed into energy errors by employing the relation

$$\delta E = C_z^{-1}\delta R_{k,\alpha}\,.$$

The coefficient C_z is the sensitivity of the respective transition energy to a variation of the nuclear charge distribution. The values of α, k, and C_z for the two transitions are given in Table VIII. Our analysis yielded NP$1s=1.52(53)$ keV and NP$2s=0.13(7)$ keV. These values are in agreement with theory. A change of the order of 10 eV in the $2p_{3/2}$ nuclear polarization correction does not significantly alter these results, justifying the use of the theoretical NP value for this level. Although the uncertainties are rather large, a nuclear polarization value of the $1s$ state of 3 keV or more is practically excluded. Such a large value is required by internal consistency for

TABLE VIII. Experimental and calculated energies of muonic transitions and their corresponding equivalent radii in ^{90}Zr.

Transition	C_z (fm/keV)		k	Experimental energy E (keV)	Calculated energy E^0 (keV)	Experimental equivalent radius $R_{k,\alpha}$ (fm)[a]
$3p_{3/2}$-$1s_{1/2}$	−0.5437	−2	2.205	3165.100(70)	3165.081	5.4690(4)
$3p_{1/2}$-$1s_{1/2}$	−0.5450	−2	2.204	3158.998(70)	3159.038	5.4693(4)
$2p_{3/2}$-$1s_{1/2}$	−0.5470	−2	2.197	2536.237(22)	2536.239	5.4684(1)
$2p_{1/2}$-$1s_{1/2}$	−0.5510	−2	2.195	2515.122(23)	2515.118	5.4683(1)
$3p_{3/2}$-$2s_{1/2}$	−0.3722	−1	2.098	522.470(24)	522.445	5.4581(9)
$3p_{1/2}$-$2s_{1/2}$	−0.3813	−1	2.097	516.419(17)	516.401	5.4583(9)
$2s_{1/2}$-$2p_{1/2}$	0.4198	−1	2.028	127.525(12)	127.522	5.4524(6)
$2s_{1/2}$-$2p_{3/2}$	0.4009	−1	2.048	106.404(9)	106.400	5.4544(4)
$3d_{3/2}$-$2p_{1/2}$	−0.3178	0	3.393	649.229(10)	649.231	5.5765(32)
$3d_{5/2}$-$2p_{3/2}$	−0.5416	0	4.131	630.533(9)	630.538	5.6462(49)
$3d_{3/2}$-$2p_{3/2}$	−0.5423	0	4.131	628.112(12)	628.110	5.6424(65)
$\Delta(2p)$	−0.7653	0	2.386	21.118(8)[b]	21.121	5.6424(65)
$2s_{1/2}$-$1s_{1/2}$	−0.6367	−2	2.223	2642.641(27)[c]		5.4709(2)
$3d_{5/2}$-$1s_{1/2}$	−0.5419	−2	2.209	3166.770(28)[c]		5.4693(2)

[a]The experimental equivalent radii $R_{k,\alpha}$ are expressed as $R_{k,\alpha}=R^0_{k,\alpha}-C_z(E-E^0)$, where $R^0_{k,\alpha}$ and E^0 are the equivalent radii and transition energies calculated with the best fit parameters of procedure (II) in Table VII, α being held fixed at 0.1029 fm^{-1}.

[b]Adopted mean value from Table VI.

[c]Derived from triangular sums of other measured transition energies.

the present experiment, if the theoretical nuclear polarization correction for the $2p$ splitting is assumed correct. Hence, the conclusions from the very general nuclear polarization correlations of Fig. 2 are confirmed.

With the constraints from such a combined analysis in mind, we fitted the muonic transition energies with different sets of parameters. First, no nuclear polarization corrections were added. If the state dependence of the nuclear polarization shift would be nearly identical to the state dependence of the finite size shift, a good fit would be expected. However, we obtained a χ^2 value per degree of freedom of 13, and in particular, a value for the $2p$ fine structure splitting which lies more than three times outside the experimental error brackets. Next, we added the theoretical nuclear polarization corrections of Table II to each muonic state before fitting again the two charge parameters c and a. The result is shown in the first column of Table VII. Although the χ^2 value per degree of freedom is reduced to 4, the calculated $2p$ splitting is again off by 2.5 standard deviations. Such a result is not surprising, following the discussion of Fig. 2(b). Finally, we took the value of the diffuseness parameter a from the (e,e) experiment of Rothhaas and the theoretical nuclear polarization corrections for the $3p$ and $3d$ states from Refs. 12 and 13 and varied the half-density radius c as well as the NP corrections in the $1s$, $2s$, $2p_{1/2}$, and $2p_{3/2}$ states. The result of this fit is shown in the second column of Table VII. The χ^2 value per degree of freedom is now smaller than 1, and the $2p$ splitting is well reproduced. The $1s$ and $2s$ NP corrections agree quite well with theory. On the other hand, the fit demands a nuclear polarization value for the $2p_{3/2}$ state larger than that of the $2p_{1/2}$ state. Taking the so obtained NP$2p$ values and varying c, a, NP$1s$, and NP$2s$ yields c and a values which deviate by not more than 1—2 am from the c and a values of the second column in Table VII. This confirms the value for the diffuseness parameter a obtained from the (e,e) data alone. The errors quoted in the second column of Table VII for the two NP$2p$ states are relative uncertainties. They were checked in different four-parameter fits. As an example, the diffuseness parameter a was fixed at its value obtained from the (e,e) data and the four parameters c, NP$1s$, NP$2p_{1/2}$, and NP$2p_{3/2}$ were varied for different values of the $2s$ nuclear polarization. The χ^2 values obtained for each minimization were then plotted as a function of NP$2s$ and the NP$2p$ limits at $\chi^2\pm1$ were extracted. A similar procedure was performed with a as a parameter. The NP$2p$ errors obtained in such a way agree with the errors listed in the second column of Table VII. In addition, the absolute values of the nuclear polarization corrections in the other states are also consistent. Hence, we adopted the nuclear parameters listed in the second column of Table VII as the "best" values.

B. Equivalent and rms radii of ^{90}Zr

It is known that a model charge distribution like the Fermi charge distribution employed above may induce slight systematical errors, specifically with regard to the rms radius.[29] Ford and Wills[30] and Barrett[31] introduced a radial moment analysis relating each experimentally measured muonic transition energy to a different generalized moment of the nuclear charge distribution. The method is based on the fact that the difference in potentials generated by the muon in the initial and the final state can be well approximated by the expression

$$V^{(i)}(r)-V^{(f)}(r)=A+Br^k e^{-\alpha r},$$

where the parameter k is a characteristic quantity for each transition and the factor $e^{-\alpha r}$ is an exponential correction factor with the parameter α usually kept constant for all transitions within the same muonic atom. For a spherically symmetric nuclear charge, each transition energy is then proportional to the "Barrett moment"

$$\langle r^k e^{-\alpha r}\rangle=\int_0^\infty \rho(r) r^k e^{-\alpha r} 4\pi r^2 dr$$
$$=\frac{3}{R_{k,\alpha}^3}\int_0^{R_{k,\alpha}} r^k e^{-\alpha r} r^2 dr .$$

The "Barrett equivalent radius" $R_{k,\alpha}$ is the radius of a uniformly charged sphere yielding the same Barrett moment as the actual charge distribution. In the present work, the parameters k and α are adjusted by the least-squares fitting program ALPHAKA (Ref. 32) until the Barrett moment corresponds precisely to the respective transition energy. In these fits, all corrections beyond finite nuclear size, and in particular the nuclear polarization shifts as discussed in the preceding section and as listed in the second column of Table VII, have been included. The equivalent radii $R_{k,\alpha}$ obtained in this way are model independent. This means that the form of the nuclear charge distribution used to calculate the respective nuclear moment affects the numerical value of this moment much less than the experimental errors. Table VIII shows in its last three columns the experimental (E) and the calculated (E^0) transition energies and the corresponding equivalent radii $R_{k,\alpha}$. The latter, labeled "Experimental equivalent radii," are determined from the equivalent radii $R_{k,\alpha}^0$ calculated with the best-fit parameters of procedure (II) in Table VII:

$$R_{k,\alpha}=R_{k,\alpha}^0-C_z(E-E^0) .$$

The parameter α has been kept constant at the predetermined value $\alpha=0.1029$ fm^{-1}. The sensitivities C_z and the moments k for each transition are also listed in Table VIII. Figure 3 shows a plot of these $R_{k,\alpha}$ values vs k. The fact that all values lie on a straight line supports the description of the nuclear charge distribution by a two-parameter Fermi distribution.[30,33] Specifically, the slope is directly related to the surface diffuseness parameter a. Deviations from a smooth line would reveal inconsistencies in the measurements themselves or in the theoretical corrections applied.

When comparing nuclear charge distributions obtained by different experimental methods like muonic atoms, elastic electron scattering, or optical spectroscopy, the root-mean-square (rms) radius is a more convenient quantity than the equivalent radius $R_{k,\alpha}$. Besides, the rms radius is a fundamental quantity of each nucleus, and is often employed in systematic analyses.[27,34,35] As already mentioned above, the rms radius obtained by fitting

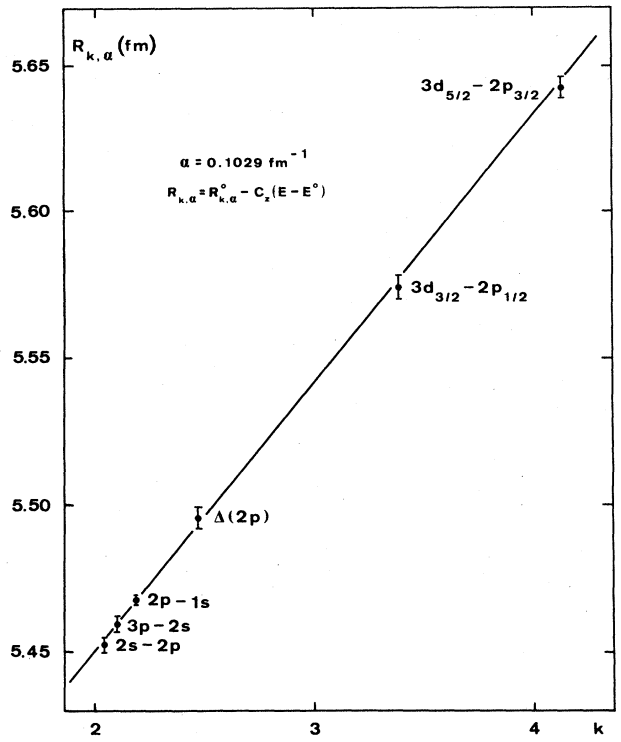

FIG. 3. Barrett equivalent radii $R_{k,\alpha}$ plotted against the moment k for different muonic-atom transitions in ^{90}Zr.

muonic transition energies alone with a two-parameter Fermi distribution, e.g., is to a certain extent model dependent. However, a combined elastic electron scattering and muonic-atom analysis provides a model-independent extrapolation from the precisely known Barrett moments of the muonic-atom transitions to the second moment $\langle r^2 \rangle$ of the nuclear charge distribution. In fact, a phase shift analysis of the elastic electron scattering data[11,36] with the Barrett moments of the different muonic-atom transitions as additional integral constraints yields the model-independent ratios

$$V_n = \frac{R_{k,\alpha}}{\langle r^n \rangle^{1/n}} .$$

In particular, the V_2 ratio corresponding to the muonic $2p$-$1s$ transitions amounts to

$$V_2 = \frac{R_{2.196,0.1029}}{\langle r^2 \rangle^{1/2}} = 1.279\,87(9) ,$$

yielding

$$\langle r^2 \rangle^{1/2} = 4.2726(9) \text{ fm} .$$

This value agrees within 0.2 am with the value given in the second column of Table VII, which has been extracted from a least-squares fit of the muonic data alone.

Table IX compares the present result for the rms radius of ^{90}Zr with other recent elastic electron scattering data[11,37–41] and the only other muonic-atom result.[42] Within the error limits, there is generally good agreement between the different measurements. The present result, based on a combined analysis of muonic-atom and elastic electron scattering data is, however, an order of magnitude more accurate. It may be employed as a reference value when measuring similar isotopes of medium-sized nuclei.

TABLE IX. Comparison of recent rms radii deduced from elastic electron scattering and muonic atom experiments.

Reference	Type of experiment	rms radius (fm)
Bellicard *et al.* (Ref. 37)[a]	(e,e)	4.1200(500)
Fajardo *et al.* (Ref. 38)[b]	(e,e)	4.2740(220)
Phan *et al.* (Ref. 39)[c]	(e,e)	4.2690
Singhal *et al.* (Ref. 40)[d]	(e,e)	4.2725
Dreher (Ref. 41)[e]	(e,e)	4.2654(35)
Rothhaas (Ref. 11)[f]	(e,e)	4.2633(84)
Ehrlich (Ref. 42)[g]	μ^- atom	4.2660(140)
This experiment	μ^- atom + (e,e)	4.2726(9)

[a]Two-parameter Fermi distribution with $c = 4.66$ fm, $t = 2.34$ fm.
[b]Parabolic Gaussian shape with $n = 2$, $c = 4.434(20)$, $z = 2.528(3)$, and $w = 0.350(25)$.
[c]Parabolic Gaussian shape with $n = 2$, $c = 4.45(5)$ fm, $z = 2.54(5)$ fm, and $w = 0.28(7)$.
[d]Three-parameter Fermi distribution with $c = 4.387$ fm, $t' = 11.094$ fm, and $w = 0.2455$.
[e]Three-parameter Fermi distribution with $c = 4.387$ fm, $t' = 11.390$ fm, and $w = 0.250$.
[f]Fourier-Bessel expansion with cutoff radius $R = 10$ fm.
[g]Two-parameter Fermi distribution.

V. CONCLUSIONS

In the present work, high precision has been obtained for those muonic-atom transition energies which are sensitive to the nuclear charge extension of ^{90}Zr. Our measurements allowed a determination of both nuclear polarization correlations and integral nuclear charge moments. With the additional input from recent elastic electron scattering data,[11,36] the rms radius of ^{90}Zr could be determined model independently and an order of magnitude more accurately than in former experiments. In addition, constraints could be set on the nuclear polarization values of the muonic $1s$ and $2s$ states. In particular, a nuclear polarization value of the $1s$ state of more than 3 keV, required in order to bring the experimentally measured nuclear polarization splitting of the two $2p$ states in accordance with theory, could be excluded. This inversion in magnitude of the two NP$2p$ values is an experimental result which until now remains unexplained by theory. The same kind of discrepancy has been observed in muonic ^{208}Pb.[6] There, an accidental unobserved resonance excitation process changing the transition energies from the two $2p$ states could still be evoked as a possible explanation. The chance that such an effect could also be responsible for the present discrepancy seems extremely remote. Hence, there seems to exist a fundamental problem in present theoretical approaches to the nuclear polarization effect. In principle, if there are magnetic polarization contributions, they could differently affect the two NP$2p$

values. However, in a second-order perturbative treatment, the energy shift does not depend on the sign of the matrix element of the residual interaction. Thus, magnetic polarization effects can be expected to have the same sign for both $2p$ states. In addition, they are not anticipated to contribute more than 10% to the splitting. Regarding the other corrections which have to be applied to the two $2p$ levels, one might question somewhat the vacuum polarization corrections of higher order $[\alpha(Z\alpha)^{n\geq 3}]$. While the calculations of Rinker and Wilets[43] are the best ones available at present, other approaches like the external field approximation method used by Calmet and Owen[44] yield slightly different results. However, uncertainties in these higher-order vacuum polarization corrections would at most influence the muonic lead data in a sensible way, but not our evaluation of μ^--^{90}Zr, since even an overestimated error of 30% in these corrections would not change our NP$2p$ values by more than the quoted relative error of ± 3 eV. Regarding the nuclear polarization corrections of the $1s$ and $2s$ states of μ^--^{90}Zr, our experiment yields results compatible with theory. The errors quoted in the second column of Table VII are of the order of 15%, considering the constraints mentioned in the caption of this table. In particular, the nuclear polarization shifts of the higher muonic states, i.e., the $3p$ states, have to be taken from theory. Although there is no reason to believe that the nuclear polarization values of higher-lying muonic-atom levels can be more reliably calculated than those of the lower levels, the absolute size of these corrections seems too small to influence our results in a perceptible way. Since this is the case for both the $1s$ and $2s$ and the two $2p$ levels, we may finally conclude that both new theoretical efforts as well as a combination of more precise muonic-atom and elastic electron scattering experiments are desirable in order to help clarify the nuclear polarization problem in muonic atoms.

ACKNOWLEDGMENTS

The authors would like to thank Prof. G. Fricke, Dr. J. Friedrich, Dr. H. Rothhaas, and Dr. G. Mallot for their valuable discussions and help regarding the elastic electron scattering data of ^{90}Zr. The authors are indebted to Dr. G. A. Rinker and Dr. Y. Tanaka for elucidating the complex theoretical aspects of the nuclear polarization corrections and their strong interest in this work. They thank Prof. H. Schneuwly, Dr. G. Piller, and M. Boschung for their help during the data-taking period, and generally for stimulating discussions. For one of us (T.Q.P.), this work was part of the requirements for his Ph.D thesis. Finally, the authors would like to thank the Swiss National Foundation for financial support.

*Present address: Institut für Mittelenergiephysik/SIN, CH-5234 Villigen, Switzerland.

[1]E. Borie and G. A. Rinker, Rev. Mod. Phys. **54**, 67 (1982).
[2]R. K. Cole, Jr., Phys. Rev. **177**, 164 (1969).
[3]M. Y. Chen, Phys. Rev. C **1**, 1167 (1970).
[4]H. F. Skardhamar, Nucl. Phys. **A151**, 154 (1970).
[5]G. A. Rinker and J. Speth, Nucl. Phys. **A306**, 360 (1978).
[6]Y. Yamazaki, H. D. Wohlfahrt, E. B. Shera, M. V. Hoehn, and R. M. Steffen, Phys. Rev. Lett. **42**, 1470 (1979).
[7]D. Kessler, H. Mes, A. C. Thompson, H. L. Anderson, M. S. Dixit, C. K. Hargrove, and R. J. McKee, Phys. Rev. C **11**, 1719 (1975).
[8]H. L. Anderson, C. K. Hargrove, E. P. Hincks, J. D. McAndrew, R. J. McKee, R. D. Barton, and D. Kessler, Phys. Rev. **187**, 1565 (1969).
[9]D. A. Jenkins, R. J. Powers, P. Martin, G. H. Miller, and R. E. Welsh, Nucl. Phys. **A175**, 73 (1971).
[10]P. Martin, G. H. Miller, R. E. Welsh, D. A. Jenkins, R. J. Powers, and A. R. Kunselman, Phys. Rev. C **8**, 2453 (1973).
[11]H. Rothhaas, Ph.D. thesis, Institut für Kernphysik, Universität Mainz, 1976.
[12]K. Tanabe, Phys. Rev. A **3**, 1282 (1971).
[13]G. A. Rinker and J. Speth, Nucl. Phys. **A306**, 397 (1978).
[14]P. Bergem, M. Boschung, T. Q. Phan, G. Piller, A. Rüetschi, L. A. Schaller, L. Schellenberg, and H. Schneuwly, Helv. Phys. Acta **56**, 974 (1983).
[15]L. A. Schaller, P. Bergem, M. Boschung, T. Q. Phan, G. Piller, A. Rüetschi, L. Schellenberg, and H. Schneuwly, Bull. Am. Phys. Soc. **28**, 997 (1983).
[16]G. A. Rinker, Comput. Phys. Commun. **16**, 221 (1979).
[17]Y. Tanaka, The formalism of MUON2 and XRAY2, Los Alamos, 1984 (unpublished).
[18]P. M. Endt, At. Data Nucl. Data Tables **23**, 547 (1979).
[19]J. Heisenberg, J. Dawson, T. Milliman, O. Schwentker, J. Lichtenstadt, C. N. Papanicolas, J. Wise, J. S. McCarthy, N. Hintz, and H. P. Blok, Phys. Rev. C **29**, 97 (1984).
[20]T. Dubler, K. Kaeser, B. Robert-Tissot, L. A. Schaller, L. Schellenberg, and H. Schneuwly, Nucl. Phys. **A294**, 397 (1978).
[21]L. A. Schaller, L. Schellenberg, T. Q. Phan, G. Piller, A. Rüetschi, and H. Schneuwly, Nucl. Phys. **A379**, 523 (1982).
[22]P. Bergem, diploma thesis, Institut de Physique, Université de Fribourg, 1982.
[23]T. Dubler, L. Schellenberg, H. Schneuwly, R. Engfer, J. L. Vuilleumier, H. K. Walter, A. Zehnder, and B. Fricke, Nucl. Phys. **A219**, 29 (1974).
[24]*Table of Isotopes*, 7th ed., edited by C. M. Lederer and V. S. Shirley (Wiley, New York, 1978).
[25]R. G. Helmer, P. H. M. Van Assche, and C. Van der Leun, At. Data Nucl. Data Tables **24**, 39 (1979); R. G. Helmer, R. C. Greenwood, and R. J. Gehrke, Nucl. Instrum. Methods **155**, 189 (1978).
[26]L. A. Schaller, D. A. Barandao, P. Bergem, M. Boschung, T. Q. Phan, G. Piller, A. Rüetschi, L. Schellenberg, H. Schneuwly, G. Fricke, G. Mallot, and H. G. Sieberling, Phys. Rev. C **31**, 1007 (1985).
[27]H. J. Emrich, G. Fricke, M. V. Hoehn, K. Kaeser, G. Mallot, H. Miska, B. Robert-Tissot, D. Rychel, L. A. Schaller, L. Schellenberg, H. Schneuwly, E. B. Shera, H. G. Sieberling, R. M. Steffen, H. D. Wohlfahrt, and Y. Yamazaki, in *Proceedings of the Fourth International Conference on Nuclei Far From Stability, Helsingør, Denmark, 1981*, edited by P. U. Hansen and G. B. Nieken (CERN, Geneva, 1981).
[28]H. Rothhaas, private communication.
[29]L. Schellenberg, B. Robert-Tissot, K. Kaeser, L. A. Schaller, H. Schneuwly, G. Fricke, S. Glückert, G. Mallot, and E. B.

Shera, Nucl. Phys. **A333**, 333 (1980).
[30]K. W. Ford and J. G. Wills, Phys. Rev. **185**, 1429 (1969).
[31]R. C. Barrett, Phys. Lett. **33B**, 388 (1970).
[32]M. Mallinger, diploma thesis, Institut de Physique, Université de Fribourg, 1982.
[33]E. B. Shera, Los Alamos National Laboratory Report LA-UR-82-1130, 1982.
[34]J. Friedrich and N. Voegler, Nucl. Phys. **A373**, 192 (1982).
[35]E. F. Hefter, M. de Llano, and I. A. Mitropolsky, Phys. Rev. C **30**, 2042 (1984).
[36]The authors are very much indebted to Dr. G. Mallot and Dr. H. Rothhaas for performing a new phase shift analysis.
[37]J. Bellicard, P. Leconte, T. H. Curtis, R. A. Eisenstein, D. Madsen, and C. Bockelman, Nucl. Phys. **A143**, 213 (1970).
[38]L. A. Fajardo, J. R. Ficenec, W. P. Trower, and I. Sick, Phys. Lett. **37B**, 363 (1971).
[39]X. H. Phan, J. Bellicard, A. Bussière, P. Leconte, and M. Priou, Nucl. Phys. **A179**, 529 (1972).
[40]R. P. Singhal, S. W. Brain, C. S. Curran, T. E. Drake, W. A. Gillespie, A. Johnston, and E. W. Lees, Nucl. Phys. **A216**, 29 (1973).
[41]B. Dreher, Ph.D. thesis, Institut für Kernphysik, Universität Mainz, 1974.
[42]R. D. Ehrlich, Phys. Rev. **173**, 1088 (1968).
[43]G. A. Rinker and L. Wilets, Phys. Rev. A **12**, 748 (1975).
[44]J. Calmet and D. A. Owen, Z. Phys. A **284**, 371 (1978).